

de Haas-Shubnikov Effect in Antimony*

J. KETTERSON AND Y. ECKSTEIN

Argonne National Laboratory, Argonne, Illinois

(Received 17 July 1963)

The oscillatory components of the transverse magnetoresistance of single crystals of antimony has been measured at 1.15°K in the range of magnetic fields from 4000–25 000 G using a derivative technique. Measurements were made for the field in the x - z , y - z , and x - y planes. Two sets of ellipsoidal carriers are clearly observed. One of the carriers was that observed by Shoenberg for which we found: $\alpha_{11}\alpha_{22}=0.334\times 10^{28}E_F^2$, $\alpha_{11}\alpha_{33}=0.563\times 10^{28}E_F^2$, and $\alpha_{11}\alpha_{23}=0.352\times 10^{28}E_F^2$. We also found for the second set of carriers $\beta_{11}\beta_{22}=0.0227\times 10^{28}E_F^2$, $\beta_{11}\beta_{33}=0.625\times 10^{28}E_F^2$, $\beta_{11}\beta_{23}=0.0424\times 10^{28}E_F^2$, and $\beta_{22}\beta_{33}-\beta_{23}^2=0.0627\times 10^{28}E_F^2$. Discussions are included relating this data to that of other experiments.

I. INTRODUCTION

ANTIMONY is a semimetal with rhombohedral crystal structure.¹ The valence of antimony is five and there are two atoms per unit cell; thus, if there were no overlap between bands, it would be an insulator. The fact that it is a semimetal is believed to be due to an overlap between the fifth and sixth bands resulting in an equal number of holes and electrons.²

Recently, the Fermi surface of antimony has been studied using the de Haas-van Alphen effect,^{3,4} ultrasonic attenuation,^{5,6} cyclotron resonance,^{7,8} infrared absorption,⁹ and galvanomagnetic measurements.^{10,11} Shoenberg concluded from his measurements of the de Haas-van Alphen effect in antimony that part of the Fermi surface consisted of a set of 3 or 6 ellipsoids having threefold symmetry about the trigonal axis. Datars and Dexter concluded that these carriers were electrons. A second set of ellipsoidal carriers which are probably holes, was first observed unambiguously by measurements of ultrasonic attenuation.^{5,6} This investigation extends the work of Ketterson⁶ to the high-field oscillatory part of the magnetoresistance, since it was clear in his investigations that, in order to find unambiguously the reciprocal mass parameters of holes, higher magnetic fields were required. The additional high-field data allows a complete determination of the parameters of the hole ellipsoids, and a more accurate redetermination of the electron ellipsoids.

II. EXPERIMENTAL METHOD

Single crystals of antimony, grown by the Czochralski method, were supplied by the Ohio Semi-Conductor

* Based on work performed under the auspices of the U. S. Atomic Energy Commission.

¹ A. H. Wilson, *Theory of Metals* (Cambridge University Press, Cambridge, 1953), p. 62.

² H. Jones, *Proc. Roy. Soc. (London)* **A155**, 653 (1936).

³ D. Shoenberg, *Phil. Trans. Roy. Soc. London* **A245**, 1 (1952).

⁴ Y. Saito, *J. Phys. Soc. Japan* **18**, 452 (1963).

⁵ Y. Eckstein, *Phys. Rev.* **129**, 12 (1963).

⁶ J. B. Ketterson, *Phys. Rev.* **129**, 18 (1963).

⁷ W. R. Datars and R. N. Dexter, *Phys. Rev.* **124**, 75 (1961).

⁸ W. R. Datars, *Can. J. Phys.* **40**, 1984 (1962).

⁹ C. Nanney, *Phys. Rev.* **129**, 109 (1963).

¹⁰ S. J. Freedman and H. J. Juretschke, *Phys. Rev.* **124**, 1379 (1961).

¹¹ S. Epstein and H. J. Juretschke, *Phys. Rev.* **129**, 1148 (1963).

Company, of quoted impurity content less than one part per million. The crystals were oriented to within 1° by Laue back diffractions x rays, and cut into rectangular parallelepipeds approximately $0.2\times 0.2\times 1$ cm with a Servomet spark cutter. Current and potential connections were made with ordinary 60/40 Pb-Sn solder and the sample was attached to the sample holder with radio cement. The current through the sample was approximately 1 A.

The magnet system used was a Harvey Wells 12-in. precision electromagnet with 2 sets of tapered 4-in. pole pieces with gaps of 0.89 and 2.6 in.; the former pole gap produced a field of 25 000 G at 50 A while the latter gave 13 800 G at the same current. The magnetic field was calibrated by a Rawson rotating coil-flux meter and precision potentiometer, the Rawson flux meter being calibrated by NMR.

A common wall-glass Dewar system of modified Hersh design was used with the high-field pole pieces, while an ordinary double glass Dewar system was used with the low-field pole pieces. The temperature of the helium bath was maintained by pumping with a Stokes-Microvac pump system and the lowest temperature obtainable with this unit was 1.15°K. All data was taken at 1.15°K.

A block diagram of the experimental setup is shown in Fig. 1. A current of 40 cps from a power amplifier was applied to a pair of modulation coils attached to each pole piece which caused a sinusoidal variation ΔH of approximately 10 G, which in turn caused a variation of the magnetoresistance ΔR . By detecting with the usual phase-sensitive detection techniques at the fundamental or second harmonic of the driving frequency, we were able to measure both the first and second derivatives of the magnetoresistance as a function of magnet current, the second derivative being employed to emphasize more rapid oscillations and to keep the envelope of the oscillations more constant as the field was raised. The output of the phase-sensitive detector was applied to the y axis of a Houston x - y recorder calibrated periodically with a potentiometer. The x axis of the recorder was driven from a precision shunt in series with the magnet current. The current in the magnet was increased by a Miller sweep gen-

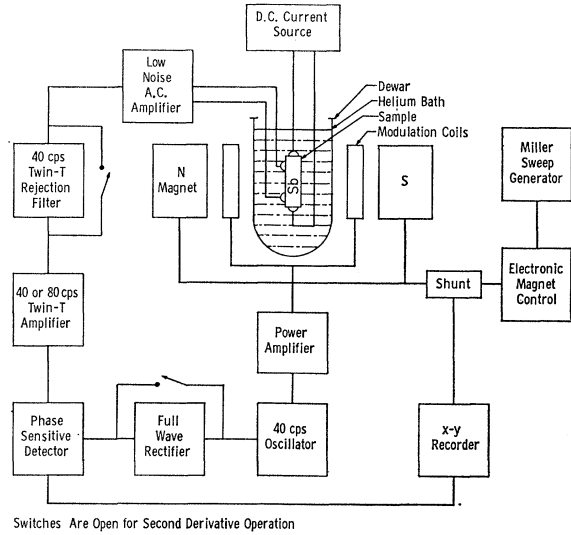


FIG. 1. Block diagram of experimental setup.

erator and the time of recording an oscillation was long compared to the time constant of the detector.

III. THEORY AND EXPERIMENTAL RESULTS

A summary of the theory of the de Haas-Shubnikov effect has been given by Kahn and Frederikse.¹² For our work all that is needed is the expression for the period given by Onsager¹³ for a general Fermi surface,

$$\Delta(1/H) = eh/ca, \quad (1)$$

where H is the magnetic field; $\Delta(1/H) = (1/H_i) - (1/H_{i+1})$ where i and $i+1$ are the maxima or minima of successive oscillations, and a is the extremal cross-sectional area of the Fermi surface in momentum space perpendicular to the magnetic field. The constants e , h , and c are, respectively, the charge of the electron, Planck's constant and the velocity of light.

We define the x , y , and z axes as binary, bisectrix, and trigonal axes respectively. The equation of the principal ellipsoid having the correct symmetry is

$$2m_0E_{F_e} = \alpha_{11}P_x^2 + \alpha_{22}P_y^2 + \alpha_{33}P_z^2 + 2\alpha_{23}P_yP_z. \quad (2)$$

The equation of the two nonprincipal ellipsoids is obtained by a $\pm 120^\circ$ rotation about the z axis, the result being

$$2m_0E_{F_e} = \frac{1}{4}(\alpha_{11} + 3\alpha_{22})P_x^2 + \frac{1}{4}(3\alpha_{11} + \alpha_{22})P_y^2 + \alpha_{33}P_z^2 \pm \frac{1}{2}\sqrt{3}(\alpha_{11} - \alpha_{22})P_xP_y \pm \sqrt{3}\alpha_{23}P_xP_z - \alpha_{23}P_yP_z. \quad (3)$$

For the hole ellipsoids, E_{F_h} will denote the Fermi

energy and β_{ij} (instead of α_{ij}) the reciprocal effective mass tensor.

The periods of the de Haas-Shubnikov oscillations may be derived by using Eqs. (1), (2), and (3). For the current $I \parallel x$, and H in the z - y plane at an angle θ from z axis, the periods are

$$\Delta(1/H)_1 = (e\hbar/cm_0E_{F_e})[\alpha_{11}\alpha_{22}\cos^2\theta + \alpha_{11}\alpha_{33}\sin^2\theta - 2\alpha_{23}\alpha_{11}\sin\theta\cos\theta]^{1/2}, \quad (4a)$$

$$\Delta(1/H)_{2,3} = (e\hbar/cm_0E_{F_e})[\alpha_{11}\alpha_{22}\cos^2\theta + \alpha_{23}\alpha_{11}\sin\theta\cos\theta + \frac{1}{4}(3(\alpha_{22}\alpha_{33} - \alpha_{23}^2) + \alpha_{33}\alpha_{11})\sin^2\theta]^{1/2}. \quad (4b)$$

For $I \parallel y$, and H in the z - x plane at angle θ from the z axis, the periods are

$$\Delta(1/H)_1 = (e\hbar/cm_0E_{F_e})[\alpha_{11}\alpha_{22}\cos^2\theta + (\alpha_{22}\alpha_{33} - \alpha_{23}^2)\sin^2\theta]^{1/2}, \quad (5a)$$

$$\Delta(1/H)_{2,3} = (e\hbar/cm_0E_{F_e})[\alpha_{11}\alpha_{22}\cos^2\theta \pm \sqrt{3}\alpha_{23}\alpha_{11}\sin\theta\cos\theta + \frac{1}{4}((\alpha_{22}\alpha_{33} - \alpha_{23}^2) + 3\alpha_{11}\alpha_{33})\sin^2\theta]^{1/2}. \quad (5b)$$

For $I \parallel z$, and H in the x - y plane at an angle θ from the x axis the periods are:

$$\Delta(1/H)_1 = (e\hbar/cm_0E_{F_e})[(\alpha_{22}\alpha_{33} - \alpha_{23}^2)\cos^2\theta + \alpha_{11}\alpha_{33}\sin^2\theta]^{1/2}, \quad (6a)$$

$$\Delta(1/H)_{2,3} = (e\hbar/cm_0E_{F_e})[\frac{1}{4}((\alpha_{22}\alpha_{33} - \alpha_{23}^2) + 3\alpha_{11}\alpha_{33})\cos^2\theta \pm (\frac{1}{2}\sqrt{3})(\alpha_{22}\alpha_{33} - \alpha_{23}^2 - \alpha_{11}\alpha_{33})\sin\theta\cos\theta + \frac{1}{4}(\alpha_{33}\alpha_{11} + 3(\alpha_{22}\alpha_{33} - \alpha_{23}^2))\sin^2\theta]^{1/2}. \quad (6b)$$

The subscript 1 refers to the principal ellipsoid and 2, 3 to the nonprincipal ellipsoids. The components of the reciprocal effective mass tensor α_{ij} are related to the effective mass tensor m_{ij} of Shoenberg by the relations

$$m_{11} = \frac{m_0}{\alpha_{11}}, \quad m_{22} = \frac{\alpha_{33}m_0}{\alpha_{22}\alpha_{33} - \alpha_{23}^2},$$

$$m_{33} = \frac{\alpha_{22}m_0}{\alpha_{22}\alpha_{33} - \alpha_{23}^2}, \quad m_{23} = -\frac{\alpha_{23}m_0}{\alpha_{22}\alpha_{33} - \alpha_{23}^2}.$$

Runs were made between 4000–25 000 G for the field in the x - y , x - z , and y - z planes of antimony. Typical data are shown in Figs. 2, 3, and 4. Figure 2 shows an example of a case where only one period is observed, and Fig. 3 clearly shows the existence of two periods. A plot of maxima and minima versus $(1/H)$ gives the value P_1 , the dominant period, while the formula $P_2 = (P_1P_0/P_1 \pm P_0)$ gives the value of the nondominant period where P_0 is the value of the beat period. The ambiguity in sign is eliminated by comparison of P_2 to the theoretical fit. Figure 4 shows an example of a faster period becoming dominant over a slower one. This phenomena of a faster period becoming dominant at higher magnetic fields occurred frequently and was

¹² A. H. Kahn and H. P. R. Frederikse, in *Solid State Physics* edited by F. Seitz and D. Turnbull (Academic Press Inc., New York, 1959), Vol. 9, p. 257.

¹³ L. Onsager, *Phil. Mag.* 43, 1006 (1952).

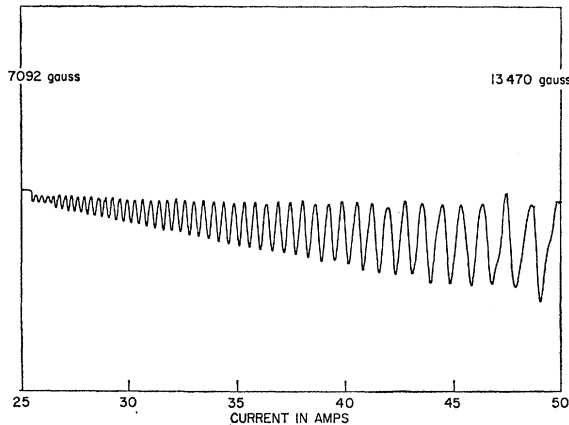


FIG. 2. Experimental curve for $\theta=160^\circ$ H in y - z plane. An orientation at which only one carrier is observed.

of considerable aid in interpreting the data. The periods observed directly and those derived using the above relation are shown in Figs. 5, 6, and 7 together with the theoretical fit to be discussed later.

Two distinct sets of carriers were observed over a greater range of magnetic field angles than in any previous experiment. Shoenberg³ observed the first of these two sets in a de Haas-van Alphen experiment, and analyzed this set on an ellipsoidal model, but he observed only a few periods of the second set. The first set was identified as electrons by Datars and Dexter⁷ in a cyclotron resonance experiment, using circularly polarized microwave power. We therefore tentatively identify the second set as holes. Both sets of carriers were observed by ultrasonic de Haas-van Alphen measurements,⁵ ultrasonic geometric resonances,⁶ and, re-

cently, by the de Haas-van Alphen measurements of Saito.⁴ In these experiments the periods of the holes were observed for only a limited range of magnetic field angles. The data of the present experiment extends through the entire range of magnetic field angles for most branches of the Fermi surface, and we were able to make a satisfactory ellipsoidal fit to the experimental data for both electrons and holes. The experimental data of previous experiments is consistent with ours for the limited range of previous observations.

1. Electrons

In fitting the electron Fermi surface we started first with the principal ellipsoid with H in the z - y plane (see Fig. 5). The procedure followed was to fit the theoretical curve $\Delta(1/H)$ [Eq. (4a)] to the experimental values of the extrema of the periods, i.e., at 36° and 126° from the z axis. These angles correspond to the magnetic field in the principal ellipse directions. Shoenberg's fit differs considerably from ours for short periods where he had no data. For example, he computes a period of $0.35 \times 10^{-6} \text{ G}^{-1}$ for H 35° from the z axis, while we measure $0.52 \times 10^{-6} \text{ G}^{-1}$ at the same angle. From our fit (using the measured tilt angle of 36°) we obtain the following three experimental parameters:

$$\begin{aligned} \alpha_{22}\alpha_{11} &= 0.334 \times 10^{28} E_F^2, \\ \alpha_{33}\alpha_{11} &= 0.563 \times 10^{28} E_F^2, \\ \alpha_{23}\alpha_{11} &= 0.352 \times 10^{28} E_F^2. \end{aligned} \quad (7)$$

By substituting these numbers in the expression for the nonprincipal ellipsoid and by comparing with experimental data, we observe that $\alpha_{22}\alpha_{33} - \alpha_{23}^2$ is small. Now,

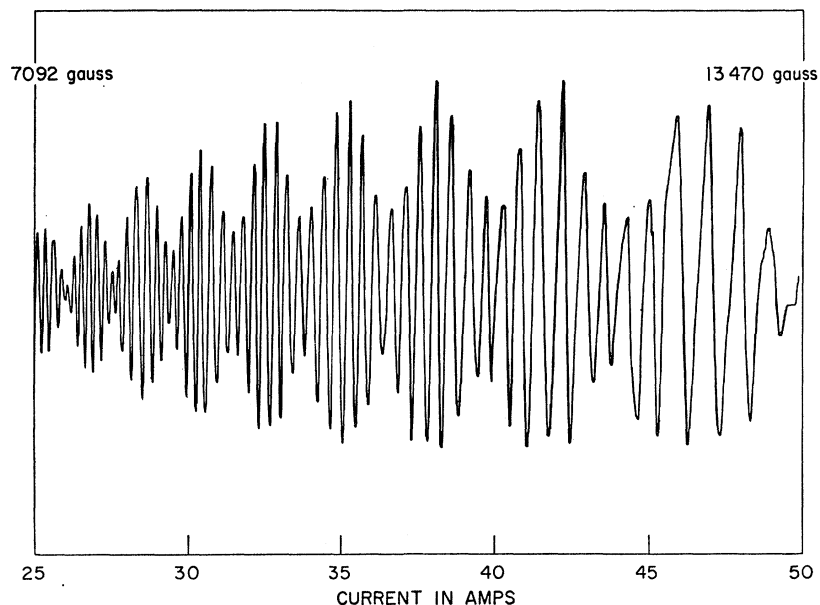


FIG. 3. Experimental curve for $\theta=75^\circ$ H in x - z plane. An orientation at which two beating periods are observed.

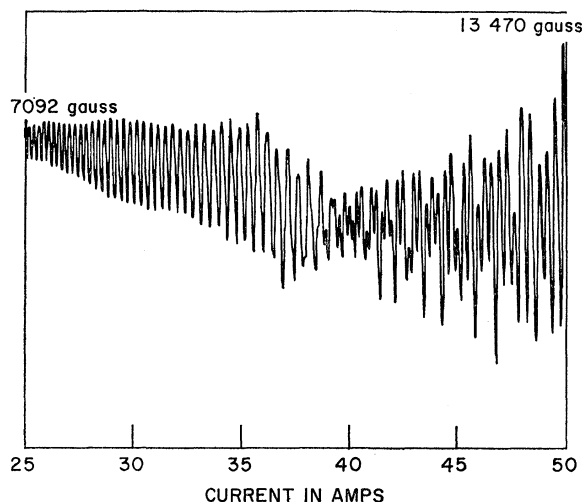


FIG. 4. Experimental curve for $\theta=0^\circ$ H in x - y plane. An orientation at which the periods of the two nonprincipal hole ellipsoids partially cancel and the period of the principal ellipsoid is observed.

going to the case where H is in the x - z plane (see Fig. 6), we plot the theoretical curves for the two nonprincipal ellipsoids, with the assumption $\alpha_{22}\alpha_{33}-\alpha_{23}^2=0$ and find that the curves fit the data quite well. We again observe that we differ considerably with Shoenberg for short periods. For example, at an angle of 40° , he calculates $0.31 \times 10^{-6} \text{ G}^{-1}$ while we measure $0.50 \times 10^{-6} \text{ G}^{-1}$ in agreement with our theoretical fit.

To compute the elements of the reciprocal effective mass tensor, we need the value of $\alpha_{22}\alpha_{33}-\alpha_{23}^2$. This combination appears alone in the period of the principal ellipsoid for $H \parallel x$ [see Eqs. (5a) and (6a)]. It can be seen from looking at the data of Fig. 6 that there are several periods in the neighborhood of $H \parallel x$, which could be assigned to the principal ellipsoid of either the electrons or holes. The period $\Delta(1/H) = 0.465 \times 10^{-6} \text{ G}^{-1}$ has been assigned to the principal hole ellipsoid for reasons to be discussed later. If Eckstein's⁵ value of $\alpha_{11} = 0.894 \times 10^{-14} E_F$ and (5a) is used, then the period of the principal electron ellipsoid should be $\Delta(1/H) = 0.518 \times 10^{-6} \text{ G}^{-1}$. A glance at Fig. 6 shows a few periods of this magnitude which are not ascribed to holes. However, a second interpretation exists, namely that the periods around $0.2 \times 10^{-6} \text{ G}^{-1}$ should be identified as due to the principal electron ellipsoid. The data of this experiment seems to favor this second interpretation, but we hasten to point out that this is in sharp disagreement with the results of Eckstein,⁵ Datars,⁸ and Nanney.⁹ The reciprocal effective masses for both interpretations are presented in Table I, where Shoenberg's value of $E_F = 18.6 \times 10^{-14} \text{ ergs}$ has been used. For the second interpretation, Priestley's¹⁴ value of the period $\Delta(1/H) = 0.227 \times 10^{-6} \text{ G}^{-1}$ for the principal el-

¹⁴ M. G. Priestley (private communication).

TABLE I. Reciprocal effective mass tensor elements.

	Electrons				
	Present experiment (Interpretation I)	Present experiment (Interpretation II)	Saito	Shoenberg	Datars
α_{11}	16.7	38.4	10	20	23.2
α_{22}	6.95	3.01	28.6	5.33	5.32
α_{33}	11.7	5.07	50.3	10.3	9.48
α_{23}	7.32	3.17	37.1	6.67	6.38
α_1'	16.7	38.4	10	20	23.2
α_2'	1.63	0.706	0.73	0.695	0.685
α_3'	17.02	7.37	78.2	14.9	14.3
θ'	36°	36°	38°	35°	36°
m_{11}	0.060	0.0260	0.10	0.05	0.043
m_{22}	0.429	0.977	0.88	1.00	0.98
m_{33}	0.250	0.580	0.50	0.52	0.55
m_{23}	-0.264	-0.611	-0.65	-0.65	-0.66
m_1'	0.060	0.0260	0.10	0.05	0.043
m_2'	0.613	1.42	1.37	1.44	1.46
m_3'	0.0588	0.136	0.013	0.0671	0.07
θ'	36°	36°	38°	35°	36°

	Holes (in units $10^{14} E_F = 1$)	
	Present experiment	Saito
β_{11}	0.445	20
β_{22}	0.0511	0.05
β_{33}	1.41	0.333
β_{23}	0.0954	0
β_1'	0.445	20
β_2'	0.0445	0.5
β_3'	1.41	0.333
θ'	4°	0°
m_{11}	2.25	0.5
m_{22}	22.4	20
m_{33}	0.815	3
m_{23}	-1.52	0
m_1'	2.25	0.5
m_2'	22.5	20
m_3'	0.709	3
θ'	4°	0°

lipoid has been used; this yields

$$\alpha_{22}\alpha_{33}-\alpha_{23}^2=0.0150 \times 10^{28} E_F^2.$$

Eckstein's⁵ value of α_{11} , together with (5a) has been used for the first interpretation; this results in

$$\alpha_{22}\alpha_{33}-\alpha_{23}^2=0.080 \times 10^{28} E_F^2.$$

The theoretical curves in the vicinity of angles at which $\alpha_{22}\alpha_{33}-\alpha_{23}^2$ dominates the period have not been plotted because of the uncertainty in this quantity.

At this point it should be emphasized that, although widely divergent values of α_{ij} have been quoted by various authors, all de Haas-van Alphen type measurements have given approximately the same values of the area. Thus, the appropriate combinations of products of α_{ij} observed by various authors are approximately equal. Table II gives a list of such combinations measured by other investigators, together with those measured in this experiment.

We feel that the method we have used of fitting the

TABLE II. Experimentally measured quantities (in units $10^{28} E_F^2 = 1$).

	Present experiment	Shoenberg	Saito
$\alpha_{11}\alpha_{22}$	0.334	0.290	0.325
$\alpha_{11}\alpha_{33}$	0.563	0.563	0.55
$\alpha_{11}\alpha_{23}$	0.352	0.447	0.443
$\alpha_{22}\alpha_{33} - \alpha_{23}^2$	0.0150 ^a	not observed	not observed
tilt angle	36°	35°	38°
$\beta_{11}\beta_{22}$	0.0227	not observed	not observed
$\beta_{11}\beta_{33}$	0.625	0.664	0.65
$\beta_{11}\beta_{23}$	0.0424	0.0525	0
$\beta_{22}\beta_{33} - \beta_{23}^2$	0.0627	not observed	not observed
tilt angle	4°	4.5°	0

^a Interpretation II. No direct observation of Interpretation I.

experimental data is preferable to a least mean-square fit because the relatively small number of experimental points in the short-period range gives insufficient weight to this range in a least mean-square fit. The advantages of using the values of the periods for H along the principal ellipse axes are that a better approximation to the volume of the ellipsoid is obtained, and the individual α_i' (the reciprocal effective mass components in the principal axes of the ellipsoid) should be less sensitive to experimental errors, including orientation errors. In addition, this procedure is less sensitive to departures from ellipticity of the Fermi surface, as it is usually more accurate to interpolate than to extrapolate. The computed values of α_i' are given in Table I.

2. Holes

It is apparent from the data that there are periods which do not fall on the curves analyzed as due to electrons; we identify these periods as due to the hole band. In particular, when $I||z$, holes are observed primarily. These are the unexplained periods observed by Shoenberg for H on the x - y plane. The period for $H||y$ and $I||z$ gives the value

$$\beta_{11}\beta_{33} = 0.625 \times 10^{28} E_F^2. \quad (8a)$$

The period for $H||z$ and $I||x$ gives

$$\beta_{11}\beta_{22} = 0.0227 \times 10^{28} E_F^2. \quad (8b)$$

The question now arises as to whether the ellipsoid is tilted. In this experiment we were not able to determine the magnetic field direction with sufficient accuracy to decide this point. Saito quotes zero-tilt angle. We have taken the tilt angle to be 4° from previous ultrasonic measurements.^{5,6} Theory shows, that in geometric resonance measurements, the orientations $q||x$, $H||y$ and $q||y$, $H||x$ should yield the same value of¹⁵ p_F^{\max} if $\beta_{23} = 0$ (where q is the sound-wave vector and p_F^{\max} the extremal Fermi momentum perpendicular to q and H); but p_F^{\max} is observed to be different for

¹⁵ See Ref. 5, formula 1a and 2a.

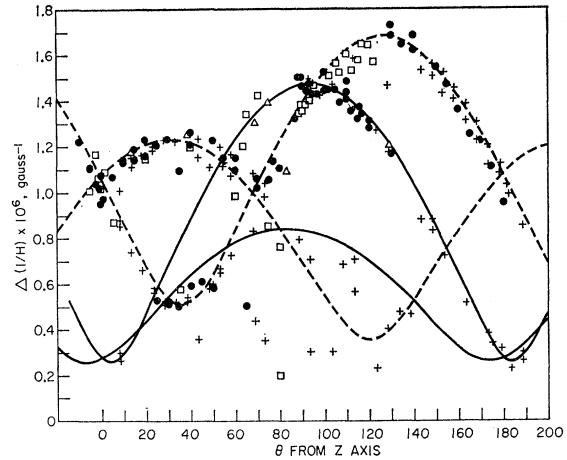


FIG. 5. Observed periods as a function of magnetic field angle for H in y - z plane with $I||x$. The dashed curves are the fit to the electron ellipsoids and the solid curves are the fit to the hole ellipsoids. Filled circles are the dominant periods (P_1) measured at low fields while squares are the nondominant periods (P_2) derived from the measured beat periods (P_0) at low fields. Crosses are high-field dominant periods and triangles are nondominant periods derived from high-field beats.

these orientations, which indicates $\beta_{23} \neq 0$. The value of 4° tilt angle was determined by using the fact that there is a sharp extremum in the ultrasonic attenuation when the magnetic field lies along a crystal symmetry axis.¹⁶ However, there is only semiquantitative agreement between the present experiment and the $q||y$ measurements in geometric resonance: Using the reciprocal masses of the present experiment, a value of $\Delta(1/H) = 1.41 \times 10^{-3} \text{ G}^{-1}$ is predicted for the period in the geometric resonance experiment with $q||y$ and $H||x$ at 60 Mc/sec, while the observed period is $1.26 \times 10^{-3} \text{ G}^{-1}$. This disagreement may be due to the fact that longitudinal transducers were used in a direction where a pure longitudinal mode cannot be propagated. Using the value of 4° for the tilt angle it is found that

$$\beta_{11}\beta_{23} = 0.0424 \times 10^{28} E_F^2. \quad (8c)$$

A few periods are observed at $I||z$, $H||x$, and several more for $I||y$, $H||x$ around $0.46 \times 10^{-6} \text{ G}^{-1}$. If these are attributed to the principal hole ellipsoid, a value of

$$\beta_{22}\beta_{33} - \beta_{23}^2 = 0.0627 \times 10^{28} E_F^2 \quad (8d)$$

is obtained. These periods are assigned to the holes rather than the electrons for the following reasons: First, if the value $\beta_{33} = 1.48 \times 10^{14} E_F$ derived from geometric resonance measurements⁵ is used, then the period is predicted to be $\Delta(1/H) = 0.49 \times 10^{-6} \text{ G}^{-1}$ for $H||x$, in close agreement with the measured value. Second, the period varies little with angle in this region, as expected for the principal hole ellipsoid in this plane. Third, the periods of the holes generally dominate

¹⁶ D. H. Reneker, Phys. Rev. **115**, 303 (1959), Fig. 9.

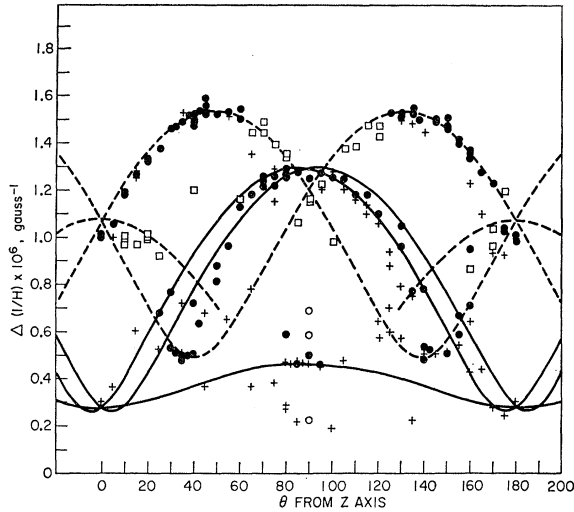


FIG. 6. Observed periods as a function of magnetic field angle for H in x - z plane with $I \parallel y$. The dashed curves are the fit to the electron ellipsoids and the solid curves are the fit to the hole ellipsoids. Filled circles are the dominant periods (P_1) measured at low fields while squares are the nondominant periods (P_2) derived from the measured beat periods (P_0) at low field. Crosses are high-field dominant periods and triangles are nondominant periods derived from high-field beats. The open circles are periods measured by Priestley.

over those of the electrons when the two are approximately equal, as can be verified by referring to Fig. 7, where it is observed that the measured periods fall definitely on the solid curve (holes) rather than the dashed curve (electrons).

The values of the elements of the reciprocal mass tensor are given in Table I. The value of β_{33} agrees well with the value $1.48 \times 10^{14} E_F$ measured in geometric resonance.⁵

IV. DISCUSSION

As was already mentioned, our data agrees well with that of Shoenberg³ and Saito⁴ wherever there is overlap. However, we find that the ratio of the maximum to the minimum period of the principal electron ellipsoid when H is in the y - z plane is 3.2, while Datars⁸ (see Fig. 5 of that paper) found a ratio of 4.58. This ratio should be the same if the Fermi surface is ellipsoidal, but this may not be the case for a nonellipsoidal Fermi surface. In addition, our observations give no indication of the heavy holes observed by Datars.

The density of carriers for holes and electrons may be calculated by using the following expression for the number of carriers per ellipsoid per cm^3 (assuming a three-ellipsoid Fermi surface):

$$n = \frac{(2m_0 E_F)^{\frac{3}{2}}}{\pi^2 \hbar^3 [\alpha_{11}(\alpha_{22}\alpha_{33} - \alpha_{23}^2)]^{1/2}}.$$

The resulting values of n_e and n_h are given in Table III. It is seen that the density of holes and electrons

TABLE III. Number of carriers.

Present experiment (Interpretation I)	Present experiment (Interpretation II)	Freedman and Juretschke
$n_e = 2.54 \times 10^{19}$ carriers/ cm^3	$n_e = 3.86 \times 10^{19}$ carriers/ cm^3	$n_e = n_h = 3.74 \times 10^{19}$ carriers/ cm^3
$n_h = 4.07 \times 10^{19}$ carriers/ cm^3	$n_h = 4.07 \times 10^{19}$ carriers/ cm^3	

is only approximately equal, and that the results agree reasonably well with the value 3.74×10^{19} carriers per cm^3 measured by Freedman and Juretschke.

The results of this experiment may now be compared with the infrared measurements of Nanney. Nanney gives the following expressions as a result of the analysis of his data, assuming ellipsoidal carriers:

$$(\mathcal{N}\alpha')_{1,2} = n_\alpha \frac{\alpha_{11} + \alpha_{22}}{2} + n_\beta \frac{\beta_{11} + \beta_{22}}{2} + n_\gamma \frac{\gamma_{11} + \gamma_{22}}{2} + \dots,$$

$$= 7.30 \times 10^{20} \text{ cm}^{-3},$$

$$(\mathcal{N}\alpha')_{1,3} = n_\alpha \alpha_{33} + n_\beta \beta_{33} + n_\gamma \gamma_{33} + \dots,$$

$$= 27.2 \times 10^{20} \text{ cm}^{-3},$$

where α_{ij} , β_{ij} , etc. are the reciprocal effective mass parameters of the various bands and n_α , n_β , etc., are the number per cm^3 of each type of carrier. Using the reciprocal electron effective masses and electron carrier concentration computed in this experiment, it is found for the first interpretation $n_e(\alpha_{11} + \alpha_{22}/2) = 3.0 \times 10^{20} \text{ cm}^{-3}$ and, for the second interpretation, $n_e(\alpha_{11} + \alpha_{22}/2) = 8.0 \times 10^{20} \text{ cm}^{-3}$. It is seen that the second interpretation more than accounts for the reflectivity, allowing no contribution from the holes.

As can be seen by looking at the experimental points

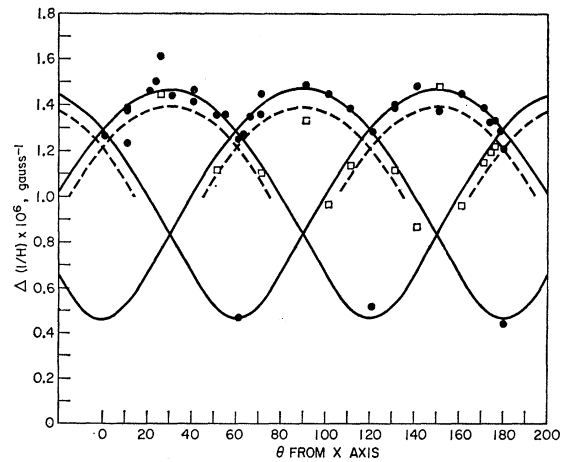


FIG. 7. Observed periods as a function of magnetic field angle for H in the x - y plane with $I \parallel z$. The dashed curves are the fit to the electron ellipsoids and the solid curves are the fit to the hole ellipsoids. Filled circles are the dominant periods (P_1) measured at low fields while squares are the nondominant periods (P_2) derived from the measured beat periods (P_0) at low fields.

of Fig. 5, there exist periods that do not fit into the present analysis. These are probably due to the existence of a third carrier. It is, in fact, quite possible that the period $\Delta(1/H) \cong 0.2 \times 10^{-6} G^{-1}$ for $H \parallel x$ is due to this third carrier. The data is insufficient to give any clear picture about the Fermi surface of these carriers; however, they may be due to the rather isotropic light hole Fermi surface observed by Datars.

V. CONCLUSIONS

Since interpretation II is in such strong disagreement with other experiments, we favor the first interpreta-

tion as being the correct one. Except for this point, there now exists a reasonably clear picture of two of the bands in antimony. Higher field measurements would aid in a more complete discussion of the other bands, and would eliminate the confusion resulting from the lack of accurate knowledge of the period of the principal electron ellipsoid for $H \parallel x$.

ACKNOWLEDGMENTS

We would like to thank Dr. M. G. Priestley and Lee Windmiller for their pulsed-field measurements. We also wish to thank Edward Yasaitis for technical aid.

Photoelectric Properties of Lead Sulfide in the Near and Vacuum Ultraviolet*

RICHARD A. KNAPP†‡

Department of Physics and Astronomy, University of Rochester, Rochester, New York

(Received 24 July 1963)

Measurements of photoelectric yield and electron energy distribution have been made on natural crystals of lead sulfide, Peruvian galena, in spherical photocells at pressures of 10^{-8} mmHg. Under these conditions maximum yields are found to be of the order of 1% in contrast to the much higher yields previously reported for this material. Yield data for cesium-coated samples are also presented, as are values of the optical absorption coefficient in the range 4–12 eV. Observed effects are interpreted as indicating the existence of an additional valence band whose maximum is located approximately 4 eV below the top of the higher bands. Such an assignment is found to be in qualitative agreement with the computed band structure.

INTRODUCTION

WHILE attempting to extend photoconductivity measurements on lead sulfide into the vacuum ultraviolet region, Smith and Dutton¹ discovered the onset, at approximately 5 eV, of an apparently very efficient external emission process. They measured yields which reached and exceeded 10% for incident energies above 10 eV and also observed unexpected changes in the energy distribution of the emitted electrons. Since such high yields are unprecedented for a material in which the electron affinity is considerably larger than the band gap² and there was some question as to the interpretation of the energy distribution data, it was thought worthwhile to conduct additional investigations.

Recent work has indicated that important band structure information may be obtained by analysis of reflectivity spectra³ and investigation of emission from

cesium coated surfaces.^{4,5} It was therefore felt that the application of such techniques to lead sulfide might provide additional information of assistance in understanding the previously observed phenomena.

EXPERIMENTAL

The monochromator, radiation source, and associated measuring equipment used in this investigation have been described elsewhere.¹ The photocell, shown in Fig. 1, is basically similar to that described by Apker *et al.*⁶ The lead sulfide emitting surface, in the form of a cleaved crystal approximately $\frac{1}{2}$ in. \times $\frac{1}{2}$ in. \times $\frac{1}{8}$ in.,⁷ is mounted rigidly at the center of the cell with the cesium source,⁸ a mixture of cesium chromate and silicon contained in a metal foil, which upon heating releases metallic cesium, directly behind it. Radiation from the monochromator enters the cell through a LiF window cemented with epoxy resin⁹ to a ground flat opposite the

* Work supported by the U. S. National Aeronautics and Space Administration (Goddard Space Flight Center).

† This paper is composed of portions of a dissertation submitted to the Graduate Council of the University of Rochester in partial fulfillment of the requirements for the degree Doctor of Philosophy.

‡ Present address: Institute of Optics, University of Rochester, Rochester, New York.

¹ A. M. Smith and D. B. Dutton, *J. Phys. Chem. Solids* **22**, 351 (1961).

² E. Taft, H. Philipp, and L. Apker, *Phys. Rev.* **110**, 876 (1958).

³ H. Ehrenreich, H. R. Philipp, and J. C. Phillips, *Phys. Rev. Letters* **8**, 385 (1962).

⁴ W. E. Spicer and R. E. Simon, *Phys. Rev. Letters* **9**, 385 (1962).

⁵ D. Brust, M. L. Cohen, and J. C. Phillips, *Phys. Rev. Letters* **9**, 389 (1962).

⁶ L. Apker, E. Taft, and J. Dickey, *Phys. Rev.* **74**, 1462 (1948).

⁷ Samples were obtained from Ward's Natural Science Establishment, Rochester, New York.

⁸ Obtained through the courtesy of Dr. W. E. Spicer.

⁹ Hysol "Epoxy-Patch" Kit No. 1-C obtained from the Hysol Company, Olean, New York.